Combination of structural monitoring and laboratory tests for assessment of Alkali-Aggregate Reaction swelling: application to gate structure dam

Alain Sellier, Eric Bourdarot, Stéphane Multon, Martin Cyr, Etienne Grimal

COMBINATION OF STRUCTURAL MONITORING AND LABORATORY TESTS FOR THE ASSESSMENT OF AAR-SWELLING

APPLICATION TO A GATE STRUCTURE DAM

A. Sellier*, E. Bourdarot, S. Multon, M. Cyr, E. Grimal

Biography: Alain Sellier is a Civil Engineering Professor at Paul Sabatier University (Université de Toulouse) and Laboratoire Matériaux et Durabilité des Constructions. He holds a PhD in Civil Engineering from Ecole Normale Supérieure de Cachan, France. His research interests concern numerical chemo-mechanical modeling of concrete structures.

E-Mail: alain.sellier@insa-toulouse.fr

Eric Bourdarot is an expert-engineer at the National Hydro-Engineering Centre of Electricité de France. A graduate of the Ecole Nationale des Ponts et Chaussées, Paris, France, he is involved in the design and reassessment of dams. In this framework, he is in charge of research and development projects in the field of durability of concrete structures. E-mail: eric.bourdarot@edf.fr

Stéphane Multon is an associate professor at Paul Sabatier University and Laboratoire Matériaux et Durabilité des Constructions (Université de Toulouse). He holds a PhD in Civil Engineering from Université de Marne la Vallée and Laboratoire Central des Ponts et Chaussées, France. His research interests concern mainly structural effects of alkali aggregate reaction.

* Correspondence to: alain.sellier@insa-toulouse.fr

E-Mail: stephane.multon@insa-toulouse.fr

Martin Cyr is an associate professor at INSA (Université de Toulouse) and Laboratoire Matériaux et Durabilité des Constructions (Université de Toulouse). He holds a PhD in Civil Engineering from INSA, France. His research interests concern cement chemistry.

Email : martin.cyr@insa-toulouse.fr

Etienne Grimal is a Civil Engineering Doctor. He is, since 2007, an engineer at the National Hydro-Engineering Centre of Electricité de France. He holds his PhD in 2007, from Paul Sabatier University in Toulouse**,** France. His work concerns the problem of dams affected by alkali aggregate reaction.

E-mail: etienne.grimal@edf.fr

Abstract

Since 1964, the Temple-sur-Lot dam, built in south west France in 1948, has been subject to continuous AAR induced displacements despite low and relatively constant alkali content in the concrete and non-significant residual swelling test results. It has been assumed that a substitution process between alkali and calcium in the AAR gel could explain this long-term behaviour. As the calcium substitution phenomenon is very slow, it cannot be detected using a conventional residual swelling test, so an original method to assess the AAR kinetics and the residual swelling capability is proposed. This method involves, firstly, a laboratory test dealing with the silica consumption kinetics and, secondly, a numerical finite element inverse analysis of the dam, which includes the consumption kinetics measured in the laboratory. The final swelling amplitude is thus fitted from only one observed structural displacement rate at a given period. The model prediction capability is validated through the comparison between the displacement of instrumented points predicted by the calculations (not used for the fitting) and the variations measured on the dam. Finally, calculations have been performed to predict the displacements and the damage fields of the dam for the coming decades.

Keywords: Alkali-aggregate reaction, swelling test, structural expertise, finite element

INTRODUCTION

Alkali-aggregate reaction (AAR) causes premature deterioration that cannot be corrected in many civil engineering structures. The expansion and cracking induced can have an effect on the functional capacity of AAR-damaged bridges and dams. Several hydraulic dams of Electricité de France (EDF) are concerned by AAR. Therefore, a behaviour model implemented in a finite element (FE) code has been developed in order to assess the safety level of the degraded structures [5-7]. The model has the particularity of representing AAR structural effects from the construction of the structure onwards. Several variables describing the advance of AAR are used, one for each range of aggregate size in the damaged concrete. These variables depend on both the degree of saturation and the temperature in the dam. First, the paper presents a historical review of the Temple-sur-Lot dam. The dam was built between 1948 and 1951 and the first cracking appeared in 1964. Several remedial work campaigns have been carried out since 1970. However, recent measurements of deformations show that expansion has continued. In a second part, the difficulty of using a conventional residual expansion test on core samples to fit the model is pointed out, particularly when the swelling rate is slow because of low alkali content in the concrete and of large aggregate sizes. Thus, the authors propose an original approach combining additional tests and physical modelling to assess the chemical AAR-advancement for each aggregate size of the damaged concrete. The chemical advancement, which is linked to the residual reactive silica content, was measured in the laboratory through expansion measurements. Then, the potential residual expansion of concrete was fitted using an inverse analysis based on an FE structural calculation that simultaneously takes into account the laboratory tests on cores drilled from the dam, the geometry of the dam, the thermo-hydro-mechanical environment of the structure, and measured displacement rates of the dam. A reliable fitting of the model was obtained by the

combination of chemical analysis performed in the laboratory and structural displacement measurements. Damage and displacements calculated on several points (not used for the fitting of the model) of the Temple-sur-Lot dam were found with an acceptable accuracy. A prediction of the dam behaviour was then made for the coming decades.

RESEARCH SIGNIFICANCE

Numerous civil engineering structures such as dams and bridges are affected by Alkali-Aggregate Reaction all over the world. The owners of the damaged structures need predictive models in order to assess the consequences of such a reaction on bearing capacity and to quantify the benefits of repairs. However, if the calculations are to be relevant, the structural model must be designed in such a way that laboratory tests and structural monitoring can be used together for the model calibration. With this in mind, the first part of the paper points out the deficiencies in the reliability of usual residual expansion tests as input data for the structural model. The second part proposes a new method based on a laboratory test and FE structural calculations to obtain model parameters.

PRESENTATION OF THE TEMPLE-SUR-LOT DAM

The Temple-sur-Lot dam, located in the south-west of France, has been operating since 1951. It includes a gate-structure dam equipped with four double leaf vertical lift gates (20 m wide, 10 m high) and a power-house with two Kaplan turbines (Figure 1 (a) and (b)). It should be noted that the dam was cast with two types of concrete mixtures (Figure 2): C_250 with a cement content of 250 kg/ m^3 (15.61 lbs/ ft^3) and containing siliceous aggregates of sizes 0-100 mm (3.94 in), and C_350 with a cement content of 350 kg/m^3 (21.85 lbs/ft^3) containing the same aggregate but with sizes 0-30 mm (1.18 in). As early as 1963, an inspection revealed the existence of cracks on the upstream part of dam piers. In the following years, difficulties in the operation of the bulkhead gates led to several interventions on the mechanical parts embedded in the concrete structure. Reinforcement of the monitoring system

provided a better description of the deformation of the piers and laboratory investigations pointed out the existence of swelling phases inside the concrete. During the period 1983-1988, extensive works were carried out on the piles, such as anchoring, and epoxy and polyurethane grouting. Recently (2002-2003), the guidance system of the gates has been modified in order to absorb concrete deformations. The effects of the swelling process on the structure are of several orders: general rising of the piers (1mm (0,04 in) / year) and tilting of the lateral piers toward the gates (0.9 mm (0.04 in) /year). Although the symmetrical movements of the central piers seem comprehensible, the horizontal movements of the lateral piers, causing some difficulty in the operation of the corresponding gates, are more difficult to understand. Several reasons have been given, in particular the existence of steel reinforcements on the external faces of the piers, the dissymmetry of the humidity conditions, or structural effects. In order to explain these particularities, make an overall evaluation of the stability of the dam, and plan its long term management, an analysis has been carried out, including a reinforcement of the monitoring system (installation of a pendulum line and a long base extensometer in the drainage gallery), laboratory investigations and FE modelling. In this respect, one of the main questions to be addressed was the estimation of the residual expansion of the concrete.

METHODOLOGY

Initially, conventional residual expansion tests [1][2][5] were carried out at LMDC for EDF according to the LPC method [17]. This method consists of measuring the longitudinal expansion and the mass variation of core samples (14 cm diameter, 30 cm length) drilled from the dam and kept in a controlled environment (38°C (100°F), relative humidity > 95%). For each type of concrete in the dam (C_350 and C_250 in Figure 2), three core samples, drilled from wet and cracked parts of the dam, were instrumented by six vertical plot lines between which longitudinal measurements were made periodically. Mean values and scatter of the

measurements are shown in Figure 3. After eight weeks, the mass was stable. During this first period, the strain variations were explained by the shrinkage reversal due to water uptake (Figure 3). So, even if a fraction of this first expansion was due to AAR [21], this part of the curve was difficult to use. After this period, the LPC method attributes the strain variations to AAR. The swelling trend is represented in Figure 3 by the dotted lines. The swelling rate is about 100 µm / m (1.2 in / ft) /year. According to the LPC recommendations, this corresponds to a negligible AAR phenomenon, which is in disagreement with the in-situ observations on the dam. Three supplementary samples were drilled from a dry part of the dam (without cracks) in order to measure the overall curve of ASR-expansion, as recommended by Multon et al. [21]. The same swelling rate was obtained [28] from both wet and dry concretes. This situation was unexpected considering that the development of AAR was not at the same stage because of the different exposure conditions of the two concretes. Therefore, the interpretation of the swelling rates by the LPC recommendations seemed unsuitable for this dam. Moreover, the tests did not give information about the residual swelling capability of the concrete since the final swelling had not been completely reached after one year (no asymptotic aspect of the curve on Figure 3). Finally, neither the final swelling amplitude nor realistic swelling kinetics were deduced from these tests. All these observations could be explained by the following considerations:

- First, the gels formed in the dam and in the accelerated tests were not of the same nature. As shown in Figure 4, products in the dam were more crystallized than the one formed in the accelerated test specimen (SEM pictures in Figure 4). This means that an accelerated test favours the formation of amorphous alkali-silica gel over more crystallized calco-alkali-silica products. This had two secondary consequences: the “molar volumes” of these two AAR-products had no reason to be the same since the chemical composition and the aspect were different. Thus, for the same quantity of reactive silica consumed in the dam and in the accelerated test, swellings could be different. The substitution process ($Na \Leftrightarrow Ca$), already

observed in [3][10][11], could be prevalent in the AAR mechanism for the dam concrete. Thus the alkali content would not be the limiting factor for the AAR-expansions and the stopping of the expansion would be driven by the total consumption of the reactive silica or the lack of calcium. However, due to the large amount of calcium in the cement paste, only the reactive silica content could be the limiting factor. So the swelling capability of the dam concrete could be deduced by quantifying the residual reactive silica in the aggregate.

- Second, core samples contained large aggregates (up to 100 mm (3.93 in) diameter) which were only superficially affected, both during the accelerated test and in the dam (Figure 5). This explains the impossibility of reaching a final swelling (usually detected by the end of swelling in the accelerated test) in a reasonable time even under the accelerated test conditions (high temperature and humidity). Hence, the dependence of the final swelling on the aggregate size must be considered with attention.

Starting from these ideas, we propose a global methodology for finding the AAR kinetics independently of the gel nature (Figure 6). As explained above, the approach is based on the assessment of reactive silica consumption. The reactive silica consumption kinetics is determined for each aggregate size range. The amplitude of final swelling is not measured from laboratory expansion tests, but assessed from an FE inverse analysis of the affected structure. The FE modelling used, the details of which are given in [6] and [7], is summarized below. It combines the advancement kinetics deduced from laboratory tests and the final AAR swelling, which is the only parameter to be fitted with the structural FE inverse analysis. Once the final swelling has been obtained by curve fitting, the numerical model is tested in order to compare its results with other expansion measurements carried out on the dam and not used for the determination of the fitted parameter. If the results are good, calculations can be carried out to predict the future structural behaviour. This global method is summarized in Figure 6.

In the following sections, the constitutive equations of the FE model are briefly summarized so as to present the main modelling assumptions. Then the experimental method used to assess the consumption kinetics of reactive silica is given. Finally, the FE inverse analysis used to fit the final swelling amplitude is illustrated and the model response is compared with the structural monitoring results.

SUMMARY OF THE FINITE ELEMENT (FE) MODELLING

The law describing the mechanical behaviour of affected concrete assumes that AAR acts on concrete through a gel pressure *Pg* which is combined with the water pressure *Pw* (Figure 7). As the pressures exist in the concrete porosity, the mechanical model is based, as in [26], on a poro-mechanical formulation described in detail by Grimal et al. [6], [7] and summarized by Eq. 1.

$$\sigma = C(\varepsilon - \varepsilon^{an}) - b_g P_g - b_w P_w \quad (1)$$

In concrete damaged by AAR, the total strain ε is induced by the AAR-gel pressure P_g acting in the concrete porosity, by the mechanical stress σ due to the structural loading and by the capillarity pressure P_w. As explained in [6] and [7], P_w represents the shrinkage mechanism. The anelastic strain ε^{an} includes both the creep strain and an irreversible strain associated with crack opening [5]. In Eq. 1, C is the damaged stiffness tensor [25]. b_g and b_w are parameters giving the influence of pressures on the concrete matrix [26].

In accordance with the above observations and previous works [4][23], it is assumed that large aggregates present lower kinetics of reactive silica consumption than small ones. Although hydroxyl, alkali, and calcium ion diffusion coefficients are nearly the same for large and small aggregates, the chemical advancement of the consumption of reactive silica, defined as the ratio of the affected zone to the sound zones of the aggregate, depends on the aggregate radius (Figure 8). That is why the size distribution of aggregates in the concrete must be discretized into several sizes (superscripts “s” in Eq 2), and a summation on

$s = \{1,..,N\}$ must be made, N being the number of size ranges. n^s is the number of aggregates of size *s* for a given size range. Thus, the gel pressure (P_g) is linked to the AAR chemical advancements A^s following equation 2:.

$$P_g = M_g \sum_{s=1}^{N} n^s \left\langle A^s f V_a^s - \left\langle V_p^s + \frac{b_g}{n^s} tr(\varepsilon) \right\rangle \right\rangle \quad (2)$$

With $\langle\ \rangle$ the positive part, V_a^s the volume of one aggregate of size '*s*' and $f V_a^s$ the maximal volume of gel created by the aggregate. A^s is the advancement of the AAR reaction for a given aggregate size '*s*'. It is defined as the fraction of the volume of AAR-gel produced at a given time by the maximal volume which can be produced by the aggregate. It evolves from 0 for the aggregate which has not yet been attacked by the reaction to 1 when the reactive silica of the aggregate has been totally attacked. It also represents the fraction of reactive silica consumed by the reaction. Therefore $n^s A^s f V_a^s$ represents the volume of AAR-gel created by n^s aggregates at a given time.

V_p^s is the available porosity connected to the aggregate "*s*" (cf. Eq. 6). $b_g tr(\varepsilon)$ is the additional connected porosity due to the concrete strain and it includes the AAR cracks through the anelastic strain (ε^{an}). The positive part symbol $\langle x \rangle = (x \text{ if } (x > 0), 0 \text{ otherwise})$ points out that the pressure P_g appears when these two porosities are filled by the gel. The coefficient M_g in Eq 2 is the bulk coefficient of the gel. The fitting of b_g and M_g, given by Grimal and al [7], requires free and constrained swelling tests to be carried out [22].

In the FE modelling, the chemical advancements A^s are computed for each aggregate size chosen to describe the aggregate size distribution. For this, a numerical step by step integration of the differential evolution equation (3) is used. This equation is inspired from [24] and [6]. It takes into account the "in situ" environmental conditions (temperature θ and water saturation degree in the pores *Sr*).

$$\frac{\partial A^s}{\partial t} = \underbrace{\alpha_{20}{}^s . \exp\left(-\frac{E_a}{R}\left(\frac{1}{273+\theta}-\frac{1}{293}\right)\right)}_{\alpha_\theta^s} \frac{\left\langle Sr - Sr^0 \right\rangle}{(1-Sr^0)} \left\langle Sr - A^s \right\rangle \quad (3)$$

With α_{20}^s the kinetic constant to be fitted, *Sr* the water saturation degree of the porosity and Sr^0 the saturation degree threshold above which the reaction occurs (estimated at 40%, according to Poyet's experimental results [24]). θ is the temperature in °C, E_a the activation energy (usually about 47000 J/M (24.748 Btu/M) [6]), and R the gas constant (8.31 J ($4.37e^{-3}$ Btu) /M.°K). This differential formulation of the AAR advancement allows environmental condition variations to be taken into account. In the Temple-sur-Lot dam, the degree of water saturation used for the integration of Eq. 3 is given in Figure 9. It was obtained from the non-linear equation of mass transfer described in [6][7][8] and solved numerically with the FE method and boundary conditions imposed from the measurements of in situ degree of saturation. The measurements of the degree of saturation were performed on nine samples (3 for each of the 3 zones of the dam) taken from the dam by dry concrete sawing. Just after the sawing, the samples were sealed in watertight packaging and the measurements of saturation degree were carried out as soon as possible. The saturation degrees were 30% in the superstructure, 45% on the external face of pile 4 and 85% in the gallery (Figure 9). Hence, the AAR relevant parameters to be fitted were: the kinetic constants α_θ^s (one per aggregate size range, $s = \{1,..,N\}$) and the AAR-gel rate *f* (related to a mineralogy type, a single one in the case of Temple sur Lot). In the following sections, the kinetic constant assessment from laboratory tests of the reactive silica consumption is first explained; then the adjustment of parameter *f* is presented.

DETERMINATION OF KINETIC CONSTANTS

Based on previous works on the effect of the size of reactive aggregates on the swelling capability of mortars [23][20], a procedure is proposed for assessing chemical advancement for each aggregate size of the concrete. This process splits the problem into two phases:

1- Aggregates of the affected concrete are first extracted by chemical attack and sifted. Then the residual reactive silica content is assessed for each reactive aggregate size using a specific procedure based on a comparative study of swelling tests of mortars. Several types of mortar containing only one aggregate size from the dam concrete are cast. The aggregates are crushed in order to obtain a same aggregate size distribution in each mortar. Moreover, a sufficient amount of alkali is added to the mortar cement paste to be sure that all the residual reactive silica contained in the crushed aggregates will be consumed during the tests. Consequently, the total swelling measured for each mortar depends only on the residual reactive silica contained in the reactive aggregate. Thus the chemical advancement of the reaction in the aggregate of the dam at the coring date can be deduced from the tests (Figure 10).

2- The constant representing the kinetics of in-situ chemical advancement (α_θ^s in Eq 3) is deduced from the chemical advancements measured for each aggregate size (A^T in Figure 10) and from the environmental conditions taken into account through the integration of Eq 3 (between the beginning of construction and the current date).

The following subsections successively develop phase 1, i.e. how the chemical advancements are assessed, and phase 2, i.e. how the kinetic constants are deduced both from the advancements and the environmental conditions.

Relationships between the chemical advancements and the residual expansions measured on mortar

As mentioned above, the principle of the test is based on the comparison between:

- residual swelling measured on mortar made with crushed aggregates extracted from the affected concrete;
- and residual swelling of mortar made with sound aggregates in order to assess the chemical advancement of the reaction in the aggregate of the dam concrete.

The "sound aggregates" can be extracted from sound zones of large aggregates (Figure 5) or can be taken in dry zones of the structure (where the AAR has not occurred). In the Temple-sur-Lot dam, these zones were the upper parts of the piles (Figure 9) where the saturation degree was lower than 40%.

The relationship between the swelling potential of mortars and the assessment of the advancement variables is based on the modelling by Poyet et al. [23]. If the alkali content is sufficient, it is assumed that a reactive aggregate with a volume V_a can create a maximal gel volume V_g (Eq 4) proportional to its own volume [23]:

$$V_g = f \cdot V_a \tag{4}$$

Several aggregate sizes can be successively studied as spherical particles. The proportionality factor *f* depends on the reactive silica content of the aggregate and on the gel texture. It is different for alkali-silica gel and calcium-silica gel. As explained by Poyet and al. [23], the gel volume can lead to swelling only if the porosity connected to the reactive aggregate (V_p in Eq 5) has been filled by the gel. The stress free swelling ε can be approximated by a linear relationship (Eq 5):

$$\varepsilon = n^s . \left\langle V_g - V_p \right\rangle \tag{5}$$

with n^s the number of reactive aggregates of size 's' per m^3 of concrete and $\langle\ \rangle$ the "positive part", as in Eq. 3.

The connected porosity is assumed to be proportional to the aggregate surface and can be idealized by a porous crown of thickness l_c (Eq 6) surrounding the spherical idealized aggregate.

$$V_p = \frac{4}{3}\pi\left[\left(R_a + l_c\right)^3 - {R_a}^3\right]p \tag{6}$$

with R_a the average aggregate radius and p the porosity of the surrounding material. When the reactive silica of the aggregate has been totally consumed by the AAR, its contribution to final stress due to free volumetric swelling is approximated by Eq (7).

$$\varepsilon^{\infty} = n \left\langle f\ V_a\ - V_p \right\rangle \quad (7)$$

with n the number of reactive aggregates per unit volume of mortar. If the aggregate under consideration has already partly reacted in the structure (before the test, i.e. between t=0, the time of construction, and t=T , the time of the test), its residual swelling potential ε^{res} in the conditions of the accelerated test (Eq. 8) depends on the chemical advancement A_T of the AAR at the extraction time T, as indicated in Eq. 8 and illustrated in Figure 10.

$$\varepsilon^{res} = n \left\langle f\, V_a \left(1 - A_T\right) - V_p \right\rangle \quad (8)$$

If A_T is close to 1, the residual swelling will be close to 0, meaning that the swelling is almost finished for the concrete corresponding to this aggregate. If A_T is close to 0, the residual swelling will be maximal.

Assessment of chemical advancement

This part presents the experimental procedure, carried out in the laboratory, that is needed to assess the residual expansion and thus the advancement A_T for each aggregate size range of each concrete of the structure. First, as mentioned in Figure 11, chemical attacks (HCl 1M for siliceous aggregates of Temple sur Lot) and sifting (Figure 12) were carried out for the two concrete types of the Temple-sur-Lot dam. In order to measure the potential for residual swelling, three mortar bars (2 cm x 2 cm x 16 cm) (0,79 in x 0,79 in x 6,30 in) were cast for each aggregate size range (each mortar in Figure 11). The division into two mortar types (N=2 in Eq. 3) for each aggregate size distribution (presented in Figure 11) was chosen to limit the number of mortars. Note that a division into more size ranges (N>2) could lead to better accuracy. Each mortar contained only a single aggregate size range of each concrete. The corresponding concrete aggregates were crushed and sifted to retain only sizes between 0.16

and 3.15 mm (0.1240 in) (Figure 11). According to previous works [23][9][19][20], smaller particles lead to smaller swelling and larger particles lead to greater but slower swelling. The total amount of crushed reactive aggregates, their size (after crushing) and the alkali content must be the same for all the mortars. An alkali content of 8 kg / 1 m^3 (0.5 lbs/ft^3) was chosen to obtain total consumption of the residual reactive silica (above this value, the final swelling becomes independent of the alkali content for this aggregate), Note that it must be also possible to ensure this last condition keeping mortar in an alkaline solution, this last procedure is currently tested in our laboratory. This choice is required so that the assumption associated with Eq 4 (total consumption of residual reactive silica) can be verified. Hence mortars differ from each other only by the residual reactive silica content of the aggregates. Thus, if one mortar presents greater swelling than another, its residual reactive silica content is larger and, according to Eq 8, its associated "in-situ" chemical advancement A_T is smaller.

After 28 days of curing in sealed bags at 20°C (68.00°F), specimens were put into a reactor at 95% RH (Relative Humidity) and 60°C (140°F). Because of the geometry of the specimens (small transversal dimensions), the mass variations stabilized a few days after the specimens had been put into the reactor and their fluctuations were negligible during the test. The longitudinal strains measured on the specimens are plotted in Figure 13. This figure shows that the concrete gravels have a greater residual swelling capability than the sands. In fact, due to the diffusion mechanism [4], alkali and hydroxyl ion ingress in larger concrete aggregates concerns only the periphery as shown in Figure 5 and symbolized in Figure 8. A large zone of unaffected silica remains at the core of the aggregate. When these aggregates are crushed before being incorporated into the mortar, most of the crushed aggregates have a low AAR average advancement. Consequently, they lead to large residual swelling (G250 in Figure 13). In contrast, the alkali and hydroxyl ion ingress concerns a larger relative zone in the sand from the concrete, where more reactive silica is reached by the ions. This leads to a large advancement in the concrete and a smaller residual swelling for the corresponding

laboratory mortars (for example S350 in Figure 13). Finally, residual swelling on mortar made with crushed aggregates showed that larger aggregates contained more unaffected silica and led to greater residual swelling than smaller ones. Moreover, Figure 13 points out that swelling capability decreases with the cement content of the concrete. The amounts of alkali and hydroxyl ions in the concretes of the dam are proportional to the cement contents. Therefore, the aggregate contained in concrete with a cement content of 350 kg/m^3 (21.8 lbs/ft^3) is more affected than the aggregate of concrete with a cement content of 250 kg/m^3 (15.6lbs/ft^3). Consequently the latter leads to smaller residual swelling (Figure 13).

It can be concluded that the chemical advancement of the AAR in each aggregate of the concrete depends on the cement content of each concrete and on the aggregate size. According to Eq 8, the consumption of silica can be divided in two parts: the first part occurs in the structure and the second part is provoked in the laboratory tests on mortars (Figure 10). The swelling curves are then used only to assess the advancement A_T of the reaction before the beginning of the accelerated test. The theoretical swelling of each mortar can be calculated using Eq 8. In this equation, all the parameters are the same for the four mortars, except the value of the initial chemical advancement A_T, which depends, as explained above, on the aggregate size and on the cement content in the concrete. In order to assess these advancements A_T, a least squares method can be used. The global error E (Eq 9) corresponding to the cumulated squared deviations between the final swellings measured on specimens ($\varepsilon_{\exp}^{res(mortar)}$) and the theoretical values computed with Eq. 8 ($\varepsilon_{th}^{res(mortar)}$) can be written:

$$E = \sum_{mortar} \left(\underbrace{n \left\langle f\, V_a \left(1 - A_T^{mortar}\right) - V_p \right\rangle}_{\varepsilon_{th}^{res(mortar)}} - \varepsilon_{\exp}^{res(mortar)} \right)^2 \qquad (9)$$

Minimizing this error leads to A_T and f given in Table 1.

As explained above, the aggregate number n in each mortar is the same for the formulations of all four mortars; it is taken to be equal to the sand content of the mortar (1500 kg /m^3 (93.5

lbs/ft^3)) divided by the absolute density of the sand and by the elementary volume of aggregate (V_a). For V_p, a characteristic length *lc* (Eq 3) of 10 µm (4e^{-4} in) was adopted in accordance with Poyet *et al.* [23].

Calculation of kinetic constant

From the structural point of view and in the FE analysis, "At" results from the integration, of the differential law of kinetics (Eq. 3) used for the computation of the chemical advancements. The temperature-dependent kinetic parameter α_θ^s in Eq. 3 is first assessed from advancements determined on the mortar tests. α_{20}^s, the kinetic constant used in the FE analysis of the dam, is then deduced from α_θ^s (Eq. 3). The relationship between the advancement A_T determined with mortar tests (A_T=A_T^{mortar} from Eq 8) and the kinetic parameter is the result of the integration of Eq. 3 (Eq. 11), from the construction time ($\tau = 0$ in Eq 11) to the time of test ($\tau = T$ in Eq 11). It takes the real environmental conditions into account: humidity through $\overline{S}_r$ (the time-averaged saturation degree) and $\overline{\theta}$ (the time-averaged temperature) of the concrete in the zone of the dam where the core samples were drilled.

$$A_T = \int_{\tau=0}^{\tau=T} \frac{\partial A(Sr(\tau),\theta(\tau))}{\partial t} d\tau \approx \int_{\tau=0}^{\tau=T} \frac{\partial A(\overline{S}r,\overline{\theta})}{\partial t} d\tau = \left[1 - \exp\left(-\alpha_{\overline{\theta}}^s \frac{\overline{S}r - Sr^0}{1 - Sr^0} T\right)\right] \qquad (11)$$

T is the age of the dam (60 years for the Temple-sur-Lot dam). A characteristic time τ^{AAR} of the reaction advancement for each aggregate type can also be defined (Eq. 12) from (Eq. 11) and linked to the "in-situ kinetic constant" α_θ^s (Eq. 13) used to assess α_{20}^s (Eq 3).

$$\tau^{AAR} = -\frac{T}{\ln(1 - A_T)} \qquad (12)$$

$$\alpha_\theta^s = \frac{1}{\tau^{AAR} \frac{Sr - Sr^0}{1 - Sr^0}} \qquad (13)$$

The characteristic time of the kinetic advancement is not explicitly used in the modelling but corresponds to the time required to reach advancement A of 63%. It is about 60 years for the C_350 sand and about 522 years for the C_250 large gravel (Table 1). These results are consistent with the observations made on the specimens. The reaction appears to be almost finished for the sand of the concrete with 350 kg/m^3 (21.8 lbs/ft^3) of cement but not so advanced for the largest gravels of the other concrete. Thus, if the alkalinity of the cement matrix is maintained in the dam, the AAR will continue. It should be noted that a reaction of substitution between the alkali of the initial AAR gel and calcium of the cement paste [12] can maintain the alkalinity condition.

ASSESSMENT OF SWELLING AMPLITUDE USING FINITE ELEMENT INVERSE ANALYSIS

The fitting between model and reality requires determination of the constant *f* (Eq 2). The constant *f* obtained from the accelerated tests (Eq 4) cannot be used for analysis of the dam because of the difference of ASR-gel nature between the long-term reaction in the dam (calcium-silica gel) and the short-term reaction in the accelerated tests (alkali-silica gel). In order to assess this constant, the model was fitted on the observed behaviour of the dam. The constant was then iteratively assessed to adjust the FE model response (in terms of structural displacements) to measurements performed on the dam. In the calculations, the final swelling of concrete containing several ranges of aggregate sizes is assumed to be the sum of the final swelling contributions of each range of aggregate size (summation on N in Eq 2). The FE model also includes the structural effects of the mechanical boundary conditions on the swelling [13][22][15][18][27]. In Eq. 3, the kinetic constants α_{20}^{s} are assessed according to the stress free expansion of the mortar (Table 1) and the environmental conditions of the dam (Eq. 11). All the other mechanical parameters needed to use the FE model were measured on drilled samples. Thus measurements of compressive and splitting tensile strengths, Young's

modulus and creep strains were carried out during the experimental study of the dam. Results are not reported here but are available in Grimal's PhD thesis [28].

The variation of the lateral displacement measured at point PC of the dam was used to fit the parameter *f* (Figure 14 and Figure 15 (a) direction yy). It was the only measurement on the dam which was used for the parameter fitting. Then, the vertical displacements of PC (Figure 15 (a) direction zz) and the horizontal displacement of PA (Figure 15 (b)) could be simulated with good accuracy. The FE structural modelling proposed in [6][7] is also able to compute the damage field in the dam due to AAR development (Figure 16). The damage variable ranges from 0 (dark zones) for undamaged material to 1 (light zones) for macroscopic cracks. Figure 16 shows the good agreement between the computed damage and the crack pattern, the lightest zones corresponding to the observed cracks (shearing crack between the two concretes, vertical cracks on the upstream part and at the bottom of the downstream part of dam piers). The lateral movement of the pile is also explained by the model with the tilting of the pier toward the gates (Figure 16). Then a prediction of the pier movements can be made for the coming decades (Figure 15 (a) and (b)) and Figure 17). Figure 15 shows that the slope of the strain tends to decrease but displacements of more than 0.020 m should be observed in the next two decades along the direction yy for PA and PC.

CONCLUSION

After the analysis of the usual accelerated residual swelling test, this paper has shown that it is difficult to use the results of such a test to predict the structural behaviour of an AAR-damaged dam. Therefore, a new method has been developed, based on two complementary fitting processes:

1- The chemical kinetics of the reaction for each range of aggregate sizes of the concrete is determined through a laboratory experimental analysis of the affected concrete. The method

used to compute the kinetic parameters of the AAR includes environmental conditions (saturation degree and temperature) of the concrete of the dam.

2- A non-linear finite element analysis of the structure is carried out to fit the final swelling amplitude of the concrete. This step takes into account one displacement rate measured on the structure and the possible heterogeneities of the environmental conditions.

To perform relevant calculations, the mechanical properties of the concrete in the structures also have to be precisely known. Measurements should be made of strength, modulus and creep characteristic. The method has been successfully tested for the Temple-sur-Lot dam. The results show that the fitting of the amplitude, using one significant displacement combined with the laboratory determination of the chemical kinetic parameters, allows other displacements of the dam and a realistic damage field to be assessed. Based on this work, a prediction of the dam's displacements and damage fields has been made for the coming decades. It shows that, although most of the displacement has already occurred, displacements and damage will continue to occur for several decades.

REFERENCES

[1] Bérubé, M.A., Smaoui, N., Côté, T., (2004) Expansion tests on cores from ASR-affected structures, Proc. 12th Int. Conf. AAR, Beijing, China, 821-832.

[2] Fasseu, P. and Mahut, B., eds (2003) Guide méthodologique : Aide à la gestion des ouvrages atteints de réactions de gonflement interne, LCPC, "techniques et méthodes des LPC" collection, Paris, France (in French).

[3] French W.J., Maintenance of mobile alkali concentration in cement paste during alkali-aggregate reaction, Enclosure to Proc. 8th Int. Conf. AAR, Kyoto, Japan.

[4] Furosawa Y., Ohga H., Uomoto T., 1994, “An analytical study concerning prediction of concrete expansion due to Alkali-Silica Reaction”, 3rd CANMET/ACI International Conference on Durability of Concrete, Nice, France, pp. 757-779.

[5] Godart, B., Fasseu, P. and Michel, M., (1992) Diagnosis and monitoring of concrete bridges damaged by AAR in Northern France, Proc., 9th Int. Conf. AAR, London, England, 368-375.

[6] Grimal E, Sellier A., Le Pape Y., Bourdarot E., “Creep shrinkage and anisotropic damage in AAR swelling mechanism, part I: a constitutive model”, accepted on 25-Jan-2008 for publication in the American Concrete Institute Material Journal.

[7] Grimal E, Sellier A., Le Pape Y., Bourdarot E., “Creep shrinkage and anisotropic damage in AAR swelling mechanism, part II : a FEM analysis” , accepted on 13-Feb-2008 for publication in the American Concrete Institute Material Journal.

[8] Grimal E., Sellier A., Le Pape Y., Bourdarot E.,"Influence of moisture and cracking on aar degradation process : impact on concrete structural behaviour using fem anlysis”, Int Conference on Concrete under Severe conditions : Environment & Loading, F.Toulemonde edt, ISSN 1628-4704, pp. 757-765, Consec 07, Tour France, 4-6 June 2007.

[9] Guédon-Dubied J.S., Cadoret G., Durieux V., Martineau F., Fasseu P., van Overbecke V., Study on Tournai limestone in Antoing Cimescaut Quarry. Petrological, chemical and alkali reactivity approach, 11th International Conference on Alkali-Aggregate Reaction in Concrete, Bérubé M.A. Fournier B. Durand B. (Editors), Quebec City, Canada, 2000, 335-344.

[10] Jensen V., Alkali Aggregate Reaction in Southern Norway, Doctor Technicae Thesis, Norwegian Institute of Tehcnology, University of Trondheim, Norway, 1993, 262 p.

[11] Lagerblad B., Trägardh J., Slowly reacting aggregates in Sweden – Mechanism and conditions for reactivity in concrete, 9th International Conference on Alkali-Aggregate

Reaction in Concrete, Concrete Society Publication CS 106, Vol 2, London, Great-Britain 570-578.

[12] Lombardi J. Perruchot A. Massard P. Larive C., "Etude comparée des gels silico-calciques produits des réactions alcalis-granulats dans les bétons et de gels synthétiques types", Cement and Concrete Research, Vol. 26, pp. 623-631, 1996.

[13] Jones A.E., Clark L.A., 1996, “The effects of restraint on ASR expansion of reinforced concrete”, Magazine of Concrete Research, 48, N°174, pp. 1-13.

[14] Larive C., Laplaud A., Joly M., 1996, “Behavior of AAR-affected concrete: Experimental data”, 10th International Conference on Alkali-Aggregate Reaction, Melbourne, Australia, pp. 670-677.

[15] Léger P., Cote P., Tinawi R., 1996, “Finite element analysis of concrete swelling due to Alkali-Aggregate Reaction in Dams”, Computer and Structures, Vol. 60, pp. 601-611.

[16] Li, K., and Coussy, O., 2002, “Concrete ASR Degradation: From Material Modeling to Structure Assessment”, Journal of Concrete Science and Engineering, V. 4, pp. 35-46.

[17] LPC. 1997 : LPC N°44 "Alcali réaction du béton : essai d’expansion résiduelle sur béton durci, à 38°C et H.R. ≥ 95%", Presse des ponts et chaussées, February 1997, in French.

[18] Malla S., Wieland M., 1999, "Analysis of an arch-gravity dam with a horizontal crack", Computers and Structures 72 (1999) 267-278.

[19] Moisson M., Cyr M., Ringot E., Carles-Gibergues A., Efficiency of reactive aggregate powder in controlling the expansion of concrete affected by alkali-silica reaction (ASR), 12th International Conference on Alkali-Aggregate Reaction in Concrete, Tang M. and Deng M. (Editors), Beijing, China, 2004, pp.617-624.

[20] Multon and al. 2008 : S. Multon, M. Cyr, A. Sellier, P. Diederich, L. Petit , “Effects of aggregate size and alkali content on ASR expansion”, submitted to ICAAR13.

[21] Multon and al. 2008 : Multon S., Barin F-X., Godart B., Toutlemonde F., “Estimation of the Residual Expansion of Concrete Affected by AAR”, Journal of Materials in Civil Engineering, ASCE 0899-1561, Vol. 20, No. 1, January 2008.

[22] Multon S., Toutlemonde F., 2006, “Effect of Applied Stresses on Alkali-Silica Reaction Induced Expansions”, Cement and Concrete Research, Vol. 36, n°5, pp. 912-920.

[23] Poyet and al. 2007 : Poyet S., Sellier A., Capra B., Foray G., Torrenti J.-M., Cognon H. & Bourdarot E., "Chemical modelling of Alkali Silica reaction: Influence of the reactive aggregate size distribution", Materials & Structures , Vol. 40, pp. 229-239, 2007.

[24] Poyet and al. 2006 : Stéphane Poyet - Alain Sellier - Bruno Capra - Genevieve Thèvenin-Foray - Jean-Michel Torrenti - Hélène Tournier-Cognon - Eric Bourdarot, “Influence of water on Alkali-Silica Reaction: Experimental study and numerical simulations”, Journal of Material in Civil Engineering, 10.1061©ASCE 0899-1561, Vol. 18 No 4 August 2006.

[25] Sellier A., Bary B. “ Coupled damage tensors and weakest link theory for describing crack induced orthotropy in concrete ”, Engineering Fracture Mechanics n°1629, May 2002.

[26] Ulm F.-J., Coussy O., Li K., Larive C., 2000, “Thermo-Chemo-Mechanics of ASR expansion in concrete structures”, J. Eng. Mech, Vol. 126, n°3, pp. 233-242.

[27] Saouma V, Perotti L, and Shimpo T, 2007, "Stress Analysis of Concrete Structures Subjected to Alkali-Aggregate Reactions", 104(5), 532-541.

[28] Grimal.E "Caractérisation des effets du gonflement provoqué par la réaction alcali-silice sur le comportement mécanique d’une structure en béton. Analyse numérique.", PhD thesis, February 7th 2007, 198 p.

Table 1: gel volume and kinetic constants for each class of aggregate size

Concrete Type	Size range (s)	Mortar type	f	A_T	α_{20}^s	τ^{AAR} (years)

C250	5-100	G250	2.%	0.12	0.0026	522
	0-5	S250		0.49	0.012	84
C350	5-30	G350		0.42	0.010	101
	0-5	S250		0.61	0.017	58

1

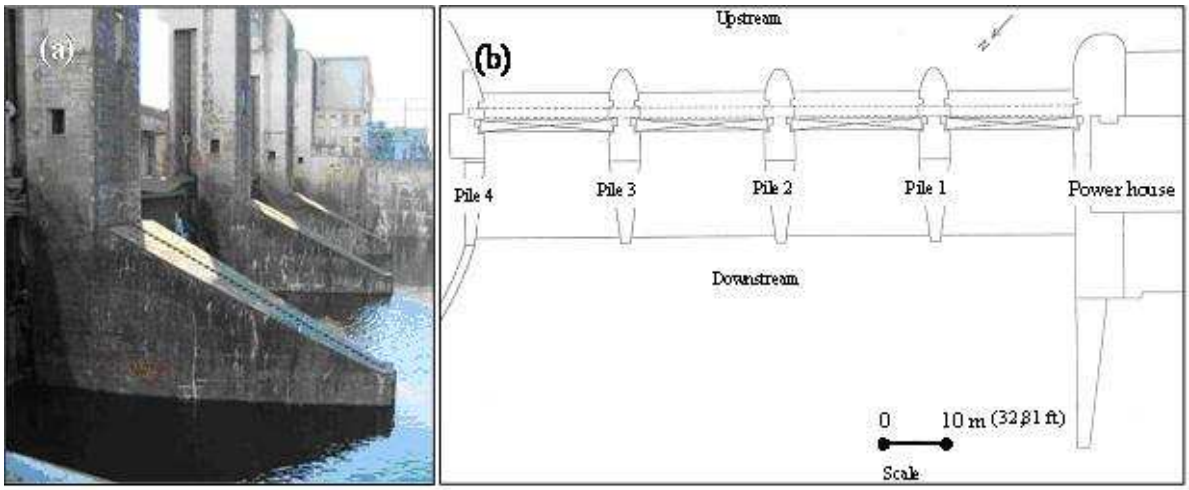

2

3 Figure 1: Overview (a) and Upper view diagram (b) of the dam

4

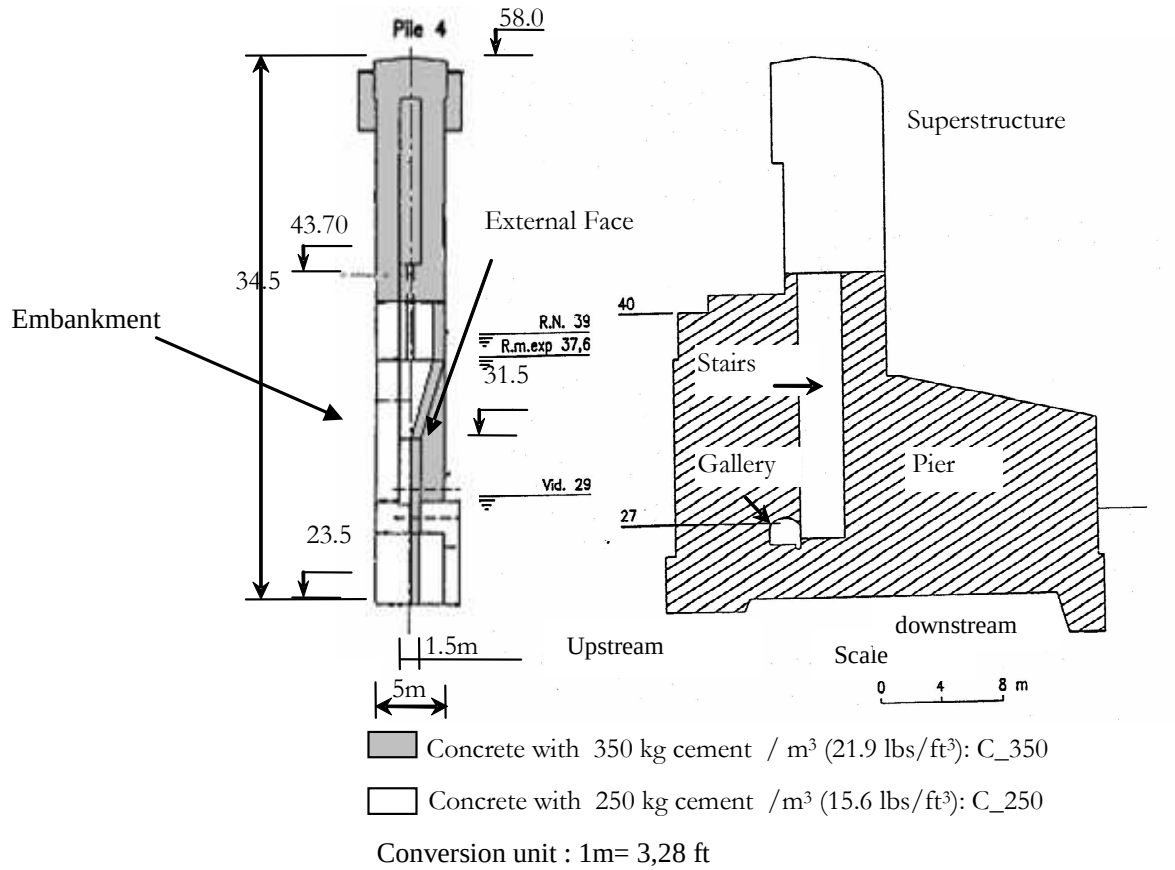

5
6

Figure 2: Downstream and transversal views of the studied pile and definition of concrete types

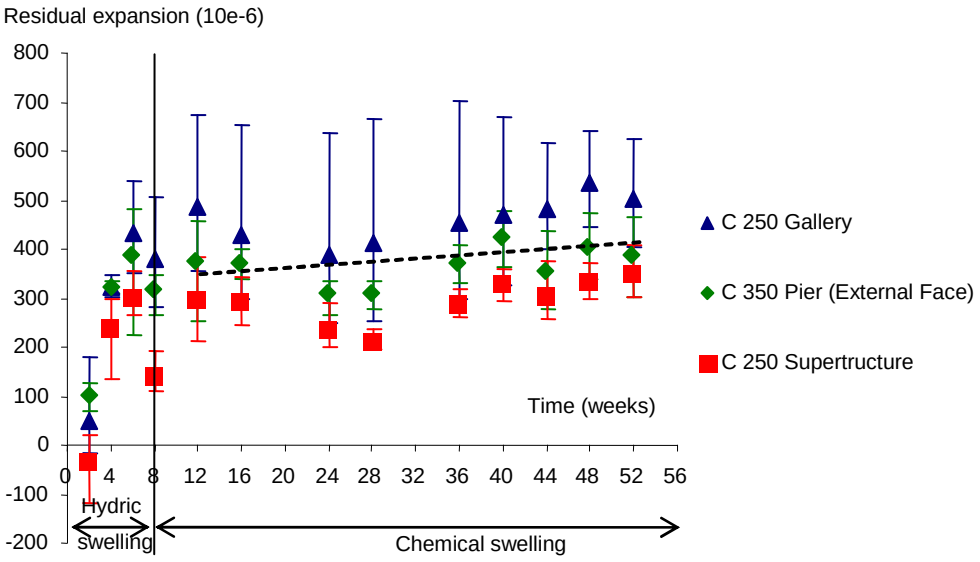

Figure 3: Longitudinal strain of core samples under usual residual swelling tests (line: experiment, dotted line: trend).

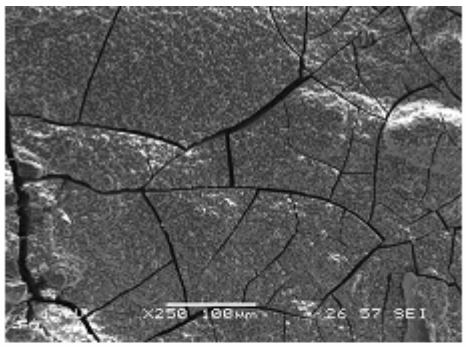

AAR product into the accelerated tests

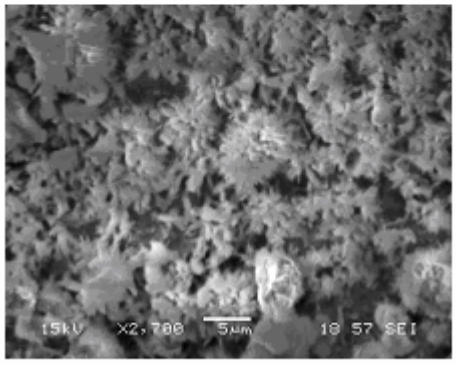

AAR product in the dam

Figure 4: AAR-gel texture differences (SEM pictures) between accelerated tests and dam

Figure 5: Peripheral zone affected by AAR in a large concrete aggregate (from a drilled core sample)

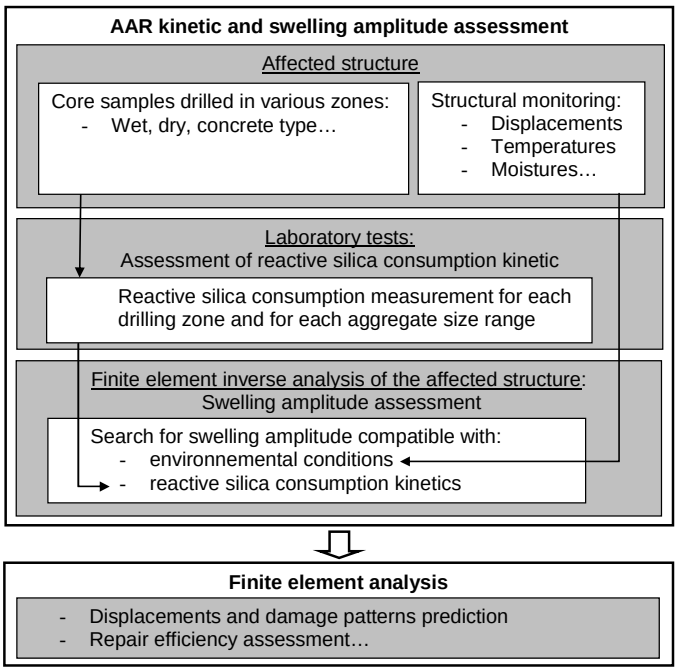

1

2 Figure 6: Global methodology summary

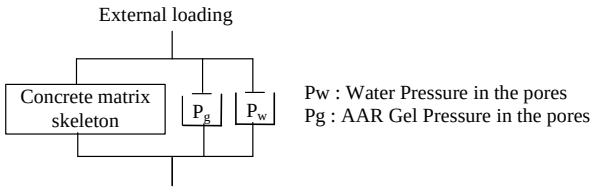

3

4 Figure 7: One-dimensional idealized view of expansive concrete behaviour model

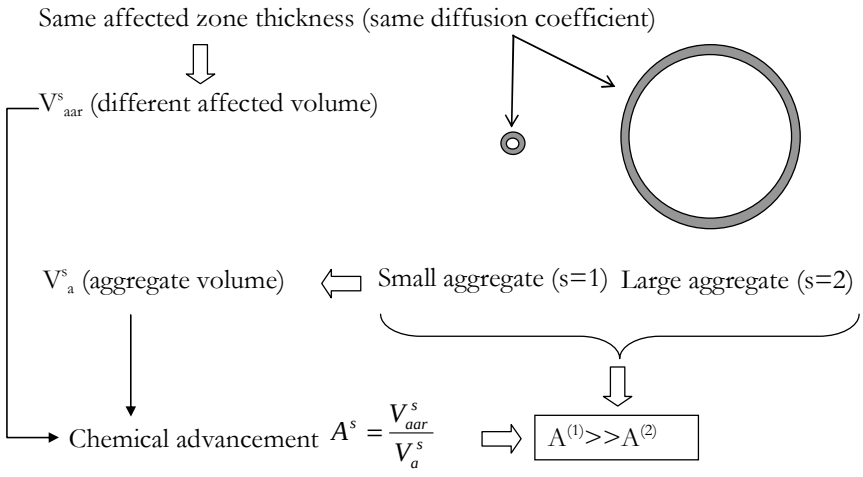

5

6 Figure 8: Difference of chemical advancement between a small (1) and a large (2) aggregate s = aggregate size

7 index

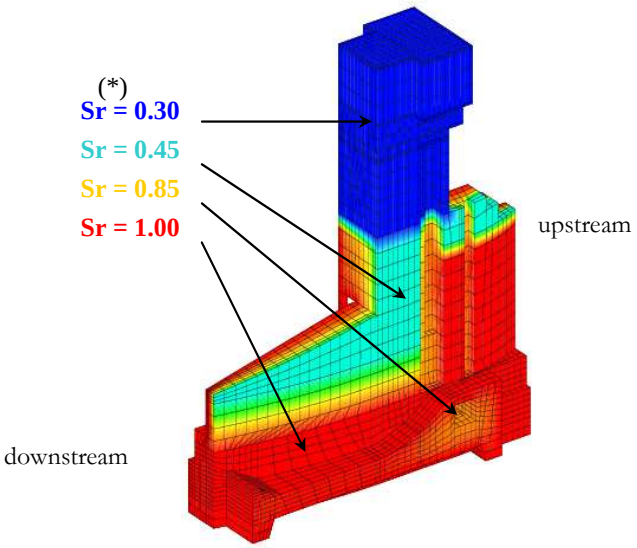

(*) boundary conditions in agreement with Sr measurements on dry sawed core samples.

Figure 9: Saturation degree field (Sr) used for the river left pile calculation.

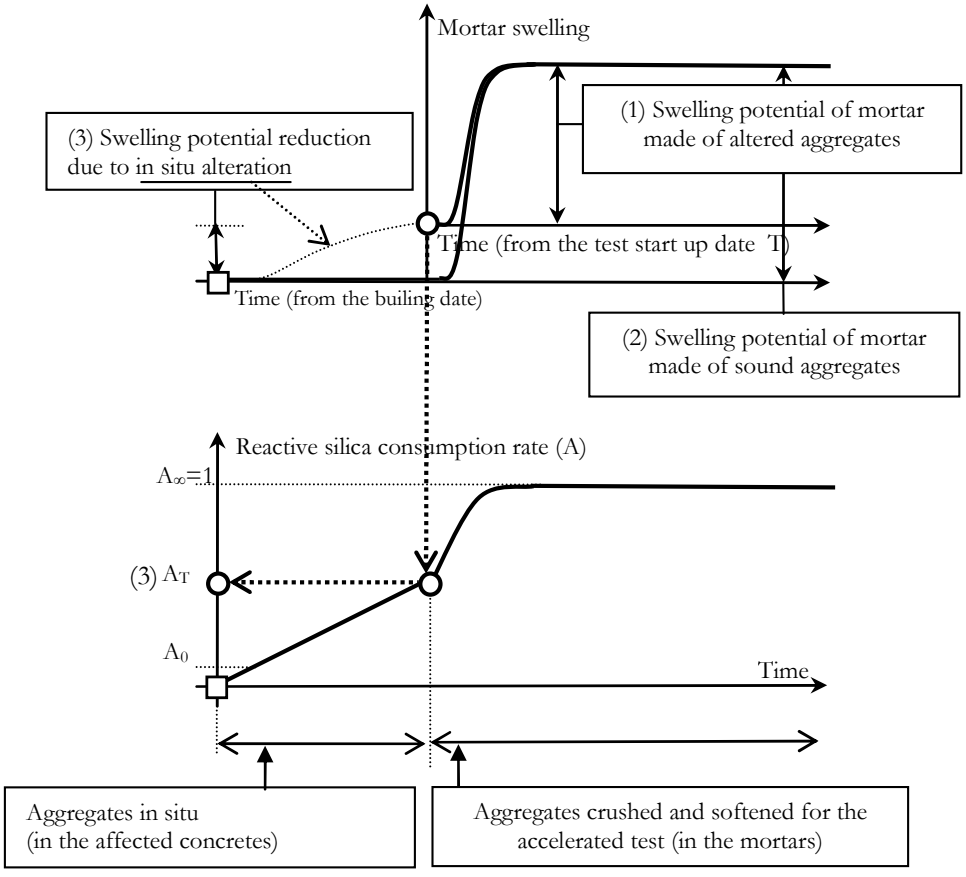

Figure 10: Principle of the chemical advancement assessment

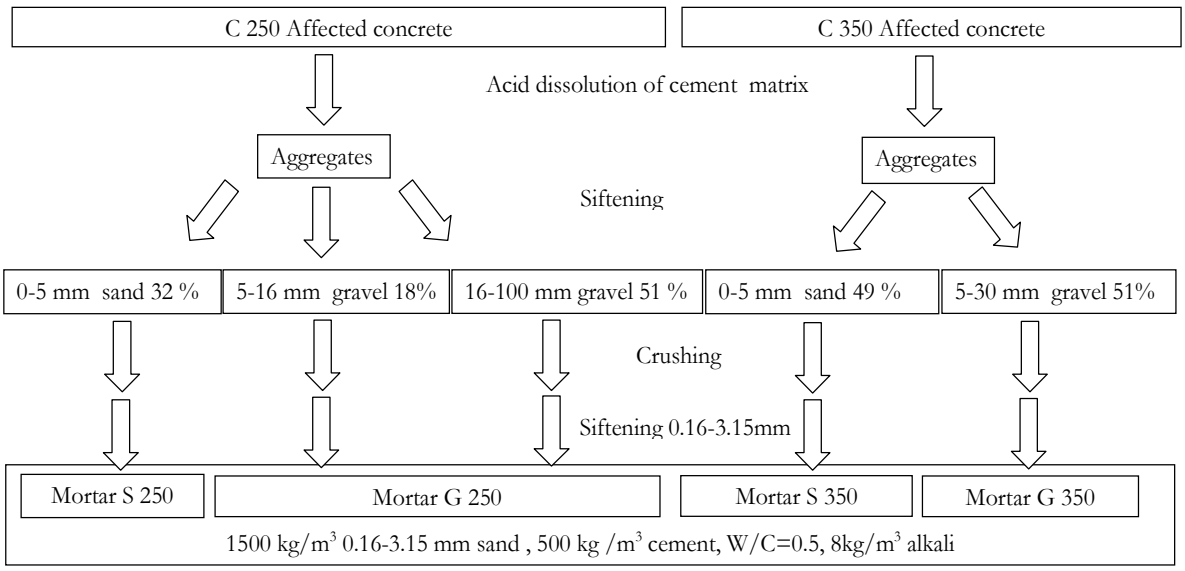

Conversion unit : 1 kg = 2,20 lbs , 1 mm = 0,0394 in, $1m^3$=35,31 ft^3

Figure 11 : Procedure of mortar fabrication for the affected concrete C250 and C350

(a) Core samples→ (b) Hydrochloric acid attack (1M) → (c)Recovered Aggregate (after sifting)

Figure 12: Aggregate extraction from a drilled core sample

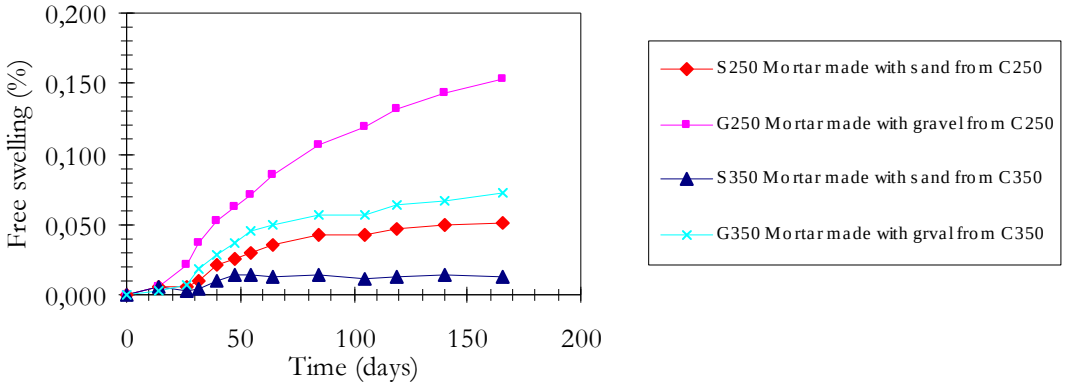

Figure 13: Swelling of mortar specimens (symbols), fitted curves (dotted lines)

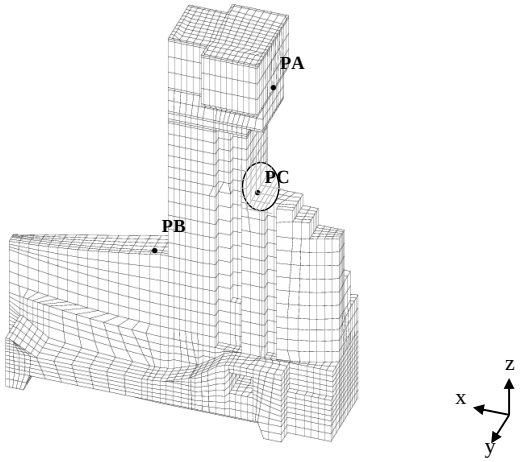

Figure 14: Mesh of the left river pile and coordinates system used. Points chosen for in situ displacement measurements

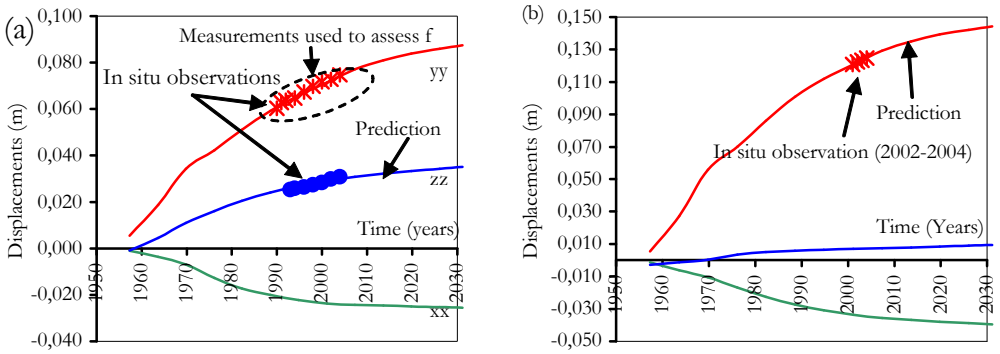

Conversion unit: 1 m = 3,28 ft

Figure 15 : (a) Fitting of the swelling amplitude on the structural displacements (point PC direction yy), prediction for PC directions zz and xx, extrapolation for the coming decades, (b) PA displacements, comparison with in situ observations and prediction for the coming decades.

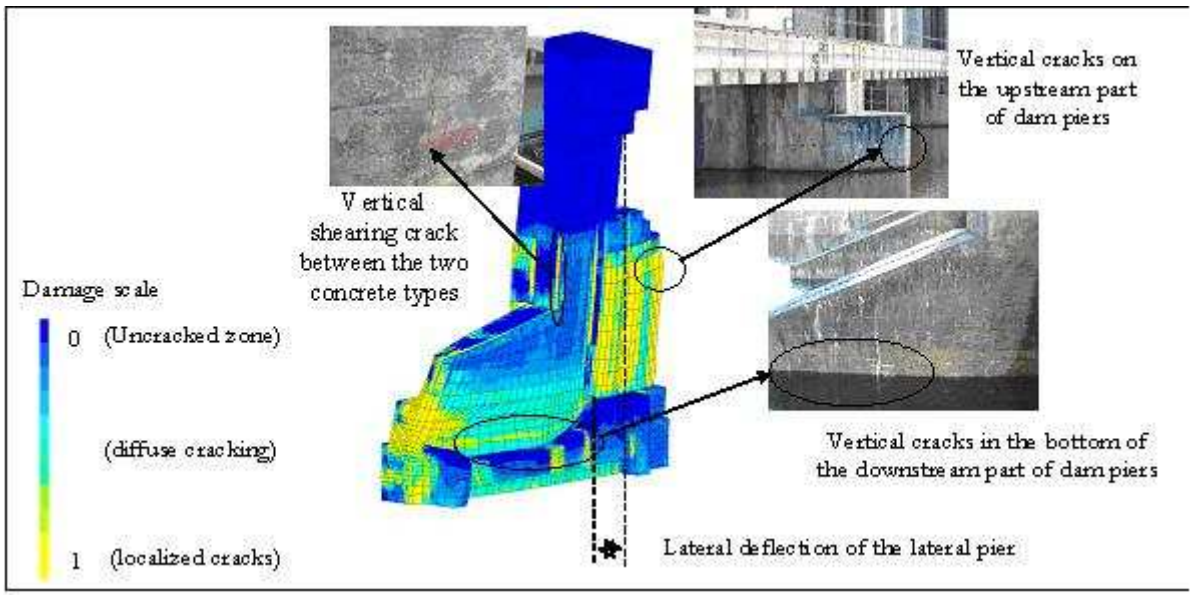

Figure 16 : Comparison between tensile damage field on deformed mesh and crack pattern observed on the dam in 2004

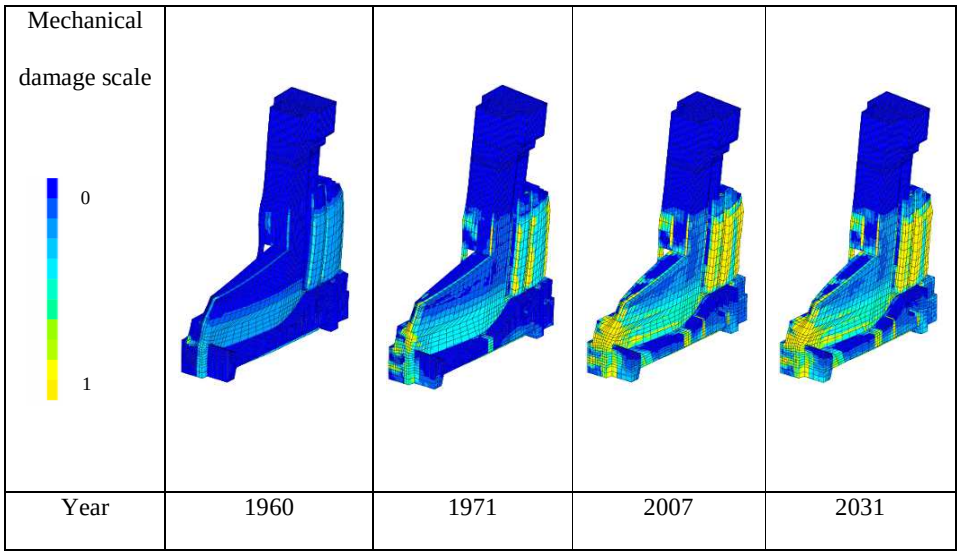

Figure 17 : Tensile damage field evolution on deformed mesh